Journal of Electroanalytical Chemistry 872 (2020) 114275

Contents lists available at ScienceDirect

Journal of Electroanalytical Chemistry

journal homepage: www.elsevier.com/locate/jelechem

On the voltage-controlled assembly of nanoparticle arrays at electrochemical solid/liquid interfaces

Cristian Zagar [a], Ryan-Rhys Griffiths [a], Rudolf Podgornik [b], Alexei A. Kornyshev [a,c,*]

[a] Department of Chemistry, Imperial College London, SW7 2AZ London, United Kingdom
[b] School of Physical Sciences, University of Chinese Academy of Sciences, and Kavli Institute of Theoretical Sciences, No.380 Huaibei, Huairou District, Beijing 101408, PR China
[c] Thomas Young Center for Theory and Simulation of Materials, SW7 2AZ London, United Kingdom

ARTICLE INFO

Article history:
Received 20 December 2019
Received in revised form 24 April 2020
Accepted 4 May 2020

Keywords:
Nanoparticles
Electrosorption
Debye screening
Image forces
Van der Waals interactions
Nanoplasmonic platforms

ABSTRACT

Research in the field of nanoplasmonic metamaterials is moving towards more and more interesting and, potentially useful, applications. In this paper we focus on a class of such metamaterials formed by voltage controlled self-assembly of metallic nanoparticale at electrochemical solid |liquid interfaces. We perform a simplified, comprehensive analysis of the stability of a nanoparticle arrays under different conditions and assembly. From the Poisson-Boltzmann model of electrostatic interactions between a metallic nanoparticle and the electrode and between the nanoparticles at the electrode, as well as the Hamaker-Lifshitz theory of the corresponding van der Waals interactions, we reach some conclusions regarding the possibility to build arrays of charged nanoparticles on electrodes and disassemble them, subject to variation of applied voltage. Since systems of this type have been shown, recently, to provide nontrivial electrotuneable optical response, such analysis is crucial for answering the question whether the scenarios of electrochemical plasmonics are feasible.

1. Introduction

The studies of solid| liquid interfaces with electrosorbed nanoparticles is an interesting new area of electrochemistry in the context of electrocatalysis and energy conversion. Recently, however, these systems found entirely novel applications as platforms for electrotuneable photonic metamaterials.

The term *optical metamaterials* is attributed to materials with odd, disruptive, often counterintuitive optical properties, the principles of operation of which are often based on subtle, nontrivial physical electromagnetic effects in nanoscale structures. An explosive development of this area was made possible with the progress in nanotechnology. Indeed, the ability to design nanostructures which control electromagnetic wave propagation revealed the potential for many interesting and useful applications, from sensors and optical switches [1] to superlenses and communication technology [2,3].[1] Many of such designed structures are built, however, fixed, and the demand to build *tuneable* metamaterials developed mainly in the investigation of electromagnetic effects that may cross-influence each other without changing the material's nano-structure [4–10]. If successful, switching the properties could be very fast. A much simpler approach would be to tune optical signals through changing the structure of the material. Well known are the attempts to do this mechanically; c.f. the material named plasmene, in which an array of metallic 'plasmonic' **n**ano**p**articles (NPs) is chemisorbed on a ribbon and stretching the ribbon one could change the optical response of the array. Generally, assembling NPs into arrays or, even more complex structures [11], leads to interesting reflectance and transmission spectra, resulting from plasmon resonances induced by light, and a way towards tuning the optical response of such systems is to tune their structures.

One way of tuning the structure of plasmonic NP arrays in real time is their voltage controlled self-assembly/disassembly at electrochemical interfaces. The idea first was proposed in Ref [12]. and later developed in a series of papers (for review see ref. [13]). Its first experimental realization has been presented in Ref. [14] for an electrochemical liquid-liquid interface, backed up by the theory of optical response spectra from such systems [15]. A detailed theory of optical spectra from the arrays of NPs at solid electrode-liquid electrolyte interfaces was presented in Ref. [16], where the presence of plasmonic substrate changes dramatically the character of the signal. Its first experimental realisation has been reported recently [17], in full harmony with theory. Let us summarize briefly the main idea of these works.

* Corresponding author at: Department of Chemistry, Imperial College London, SW7 2AZ London, United Kingdom.
E-mail address: a.kornyshev@imperial.ac.uk (A.A. Kornyshev).

[1] A reference added in proof, in view of the current exceptional interest to virology:
A.M. Wen, R.Podgornik, G.Strangi, N. F. Steinmetz, Photonics and plasmonics go viral: self-assembly of hierarchical metamaterials, *Rendiconti Lincei - Scienze Fisiche e Naturali*, **26**,129–141 (2015).

http://dx.doi.org/10.1016/j.jelechem.2020.114275

In an electrochemical liquid-liquid cell, at the interface of two immiscible electrolytic solutions [18] (say NaCl in water and TBA-TPB in 1,2, dichloroethane), plasmonic NPs, say AuNp-s, adsorb at the interface, piercing it, to block the unfavourable surface between water and oil. If the surface energy of a NP in contact with water and with oil is lower than the surface energy of that blocked interface area, there will form a so-called capillary well that will keep such NP at the interface [19]; such NPs which are dissolved exclusively in water will get adsorbed at the interface. But NPs from the very beginning are functionalized by ligands the head groups of which dissociate in water and leave ligands charged – for mercaptanoic acid, negatively charged. Functionalization is needed to ensure colloidal stability of NPs in aqueous electrolyte bulk, otherwise they will fuse due to Van der Waals forces. The strength of thus provided electrostatic repulsion is controlled by two factors: (i) electrolyte concentration (inorganic electrolyte in water and organic electrolyte in oil) – the higher concentration provides the Debye screening of electrostatic interactions; (ii) the net charge of ligands on the NP (usually controlled through pH). But somehow, since we made NPs repel each other, they will tend not to assemble closely to each other when adsorbed at the interface. And this is exactly what we see experimentally, either through X-ray characterisation of the NP arrays at the interface, or through their optical reflectivity [20] (the reflection is stronger for denser arrays, and the overall spectrum changes: maximum reflectivity shifts to the red in full accordance with the developed theory [15]). In order to make the array denser for a given pH and electrolyte concentration, one needs to increase the driving force for each particle to get adsorbed at the interface. One way to do it, is to apply voltage across the interface in an electrochemical cell, i.e. polarise aqueous phase more relative to oil. This was shown to be perfectly reversible, allowing voltage-controlled formation of NP arrays at liquid-liquid interfaces, and thereby building the first electro-tuneable/switchable mirror [14].

Liquid/liquid electrochemical interfaces have a lot of interesting features and advantages, but since it is hard to maintain those interfaces vertical, solid-liquid systems are of special interest. These can be of two kinds:

- Solid transparent electrode [e.g., Indium Tin Oxide (ITO)] in contact with aqueous electrolyte solutions.
- Metal electrode in contact with aqueous electrolyte solutions.

The first class of systems will function similar to the liquid | liquid one. Polarizing the electrode positively, it will force negatively charged NPs to get adsorbed at the interface to form a dense array and thereby provide a mirror function; polarizing the electrode negatively will push NPs away, into the bulk, thus making the interface transparent.

The second class of systems behave entirely differently, and in two possible ways, depending on the material of the substrate metal and of the NP. First of all, when NPs are not adsorbed on the solid substrate, the latter is a mirror. If it is gold, the mirror is not perfect, but having adsorbed a homogeneous array of AgNp-s make its reflection spectrum flatter, more uniform. If the substrate is silver, and NPs are AuNp-s, the effect is opposite, always a perfect mirror gets a broad dip in reflection spectrum, i.e. mirror is acquiring a colour, and the denser the array of AuNPs, the stronger the dip and the corresponding colour change, as predicted by the theory [16] and confirmed by experiment, in full agreement with the theory [17].

More systems of this kind can be envisaged [13,21], but all can be categorized as *electrochemical plasmonic* (EP) systems. A few details on solid/liquid EP-systems should be mentioned before focussing on the subject of this paper.

The speed of response to changed voltage, so far demonstrated was very slow, but… expectedly slow. Indeed, the capillary well at the interface extends just over the Debye length in electrolyte. So, if particles are left dispersed in the bulk of a macroscopic solution and in amounts to just cover the interface, it may take hours for them to randomly diffuse toward the surface and get trapped in the well. When, however they leave the well, the array loses its coherence very fast, and the mirror function disappears. The kinetics of NP adsorption in macroscopic systems have been experimentally studied for both liquid|liquid [14] and solid|liquid [17] systems, in full agreement with theoretical expectations. It was made clear that if the adsorption kinetics is fully controlled by diffusion of NPs from the bulk, there is a very simple recipe how to speed it up: the time for reaching the interface is roughly inversely proportional to the square of NP concentration. The way to increase the latter without making the solution coloured was to decrease the thickness of the aqueous phase. That effect has been studied and the one-over-square-root-of-concentration law was approved. Thus, the way to reach a millisecond response time was straightforward: build a micro-or nanocell.

It remained, however, to be understood, under which conditions adsorption and desorption of NPs are diffusion controlled, and what is basically the balance of forces that brings NPs to or pushes them away from a neutral or polarized electrode. Next, we need to understand how such NPs would interact with each other at the interface, and what the coverage dependence on applied voltage, concentration of electrolyte and the charge of functionalized NPs will be in the end. Whereas for liquid|liquid systems a more primitive theory of this kind has been developed [12,22], which justified the principle possibility of electrovariable plasmonics, this has not been done for solid|liquid interfaces.

The latter task is the main subject of the present paper. It attempts to give a first theoretical basis on whether voltage-control over the density of the adsorbed NP arrays at solid electrodes is, in principle, possible, which is the foundation of electrochemical plasmonics at solid electrodes. Such a study is also expected to reveal the means for the fine tuning of such control, through adjusting electrolyte concentration and ionization of ligands, as well as explore the effect of the size of NPs.

Note that generally the theoretical machinery of electrochemical plasmonics is comprised of three main components.

- The theory of stability of NP arrays at a polarised electrode, characterised by an equilibrium electrosorption isotherm, based on the theory of interactions of NPs with the electrode and with each other.
- The theory of NP adsorption/desorption kinetics, based on a quasi-steady state approximation for diffusion and an adsorption isotherm for surface coverage that has common elements with the theory of adsorptions kinetics of (macro)molecules.
- Electrodynamic multilayer stack model, which can quickly provide the optical response of NP arrays assembled near (generally, film-covered) substrates, for a given structure of the array, size, shape, and material of NPs, and their disposition with respect to the substrate.

The third component is well developed [15,16], giving excellent results as compared to numerical COMSOL simulations, but taking seconds to get the full spectra, with the transparency of results, which allows to avoid the 'black-box' simulations. The second component can be based on the adjustment [17] of existing kinetic theory of adsorption [23]. But the first component is the least, if at all developed, and the present study makes the first steps in this direction.

The last comment before we begin is that we will consider different electrodes, transparent ITO type, or metallic, like gold and silver, but considering the latter we may need to assume a protective layer on them, such as e.g. TiN, of SAMs, which are often used to avoid oxidation of surfaces, or passivate the electrode against water electrolysis or electrochemical reactions of ions of electrolyte for the applied electrode potentials.

2. Electrostatic vs Van der Waals forces

Two main effects will be accounted for: electrostatic and Van der Waals interactions.

As mentioned previously, metallic NPs in solution always exhibit attractive van der Waals interactions, which are strong enough to force them to agglomerate into clusters. Stabilising the solution is, therefore, crucial, and is achieved by functionalising NPs with ligands that can ionise. Usually, these ligands are mercaptanoic acids, which lose protons from their carboxyl groups and become negatively charged. Ionisation of ligands may, therefore, create enough charge on the surface of the particles that electrostatic repulsions would stop them from aggregating. Under these

conditions, the strength of interaction of the charged NPs can be adjusted by changing only two 'chemical' parameters. First, pH is what controls the fraction of dissociated ligand molecules directly. By increasing the pH, the number of ionised ligand molecules also increases, so NPs have more charge attached to them and repulsion becomes stronger. The second parameter is electrolyte concentration. The higher the concentration, the weaker the electrostatic repulsion becomes. Usually the balance between pH, electrolyte concentration and, sometimes NP concentration as well, is found experimentally, and there is not much flexibility left in these parameters once the solution is prepared.

Description of electrostatic interaction of NPs in solution with the interface and each other near the interface is a tricky task, as it involves the response of the metal substrate, i.e. image forces, also screened by electrolyte ions. Furthermore, when the electrode is polarized, an electrical double layer will be formed at the interface, and the electric field within the double layer will act on the charges of NPs. We will explore the simplest possible approximation to the solution of this problem, considering those charges fixed, as well as ignoring the polarizabilty of the particles. Note, furthermore, that we will not be involved here in more complicated theory that allows for like-charge repulsion, because we will not be considering electrolytic solutions with large Bjerrum lengths, dealing exclusively with 1–1 aqueous electrolytes, as experimentally most practical in electrochemical plasmonics [14,17]; thus, electrostatic interactions between nanonoparticles that are charged in the same way will be solely repulsive.

When considering Van der Waals interactions of nanoparticles with electrodes we will use standard expressions of the Lifshitz theory [24]. But when considering Van der Waals pair interactions between NPs, we will neglect the effect of the substrate on these interactions. This will likely slightly overestimate the attractive Van der Waals force between the NPs. The theory of interaction of two metallic spheres of finite radius near a flat metallic substrate is cumbersome and not fully developed, but from the theory of point-like fluctuating dipoles near metal substrate [25–27] we know the effect of such substrate will be in reducing the Van der Waals attraction.

All these calculations will be performed to figure out (within the mentioned theoretical framework) whether spontaneous assembly or disassembly can be induced by changing voltage and, furthermore, to show how the surface NP population responds to its change.

3. Model assumptions and basic equations

The simplest and most natural way of describing a solid-liquid interface is by modelling it as a plane which separates two semi-infinite media, namely an aqueous electrolyte and a solid metallic or semi-metallic material. Geometrically, this approach works under two conditions, that should be fulfilled in practice. First, the quasi-flat approximation is adequate only if the surface roughness is small. In this case, small implies it is practically flat down to the nanoscale. Second, the semi-infinite description is reliable only if the electric fields present in the system do not reach the physical end of the solid or liquid phases. Theoretically, this happens if the characteristic screening lengths in the two phases are short compared to the size of the system. For the aqueous phase, electrolyte concentrations are typically within 10–100 mM, leading to Debye screening lengths of the order of nm, which stop electric fields from propagating towards the physical boundaries of the system. Regarding the solid phase, electrons tend to screen the electric fields very efficiently. A simple estimate of this capability can be done with the help of the so-called Thomas-Fermi screening theory. For a metal, the screening length is extremely small, on the order of one A, or even less. This is caused by the very loose binding of the electrons in the conduction band and it makes those electrons move almost freely within the structure. For a semi-metal, electrons are bound more tightly, leading to an increase in Thomas-Fermi length to the order of a few nm. Even in this case, unless we deal with an electrochemical 'nano-cell' [28], the system remains big enough to screen the fields completely.

Below, the main types of interactions – electrostatic and van der Waals, are treated independently, and their contributions added towards the overall effect. Considering this is a verified approach for soft interfaces [29], it also should, in principle, give at least an estimate of the energies present in the system. In the following sections, two phases, aqueous and solid, will be named phase 1 and phase 2, respectively, and the variables and constants associated with them will be labelled accordingly. Full derivations of the electrostatic interactions are also given in the Supplementary Information (SI).

3.1. Electrostatic interactions

The most common way of modelling electric potentials in electrolytes and electrolyte-like systems is the Poisson-Boltzmann Eq. [30]:

$$\nabla^2\phi + \sum_i \frac{z_i\nu_i ec}{\epsilon_0\epsilon_1}\ \exp\left(-\frac{z_i e\phi}{kT}\right) = -\frac{\rho}{\epsilon_0\epsilon} \tag{1}$$

where ϕ is the electric potential, as a function of coordinates, z_i-the valence of ion i, ν_i-number of ions per molecule of electrolyte (i.e., stoichiometric coeffecient), e is the elementary charge, c is electrolyte concentration, kT is thermal energy, ϵ_0 and ϵ are the permittivity of the vacuum and dielectric constant respectively, and ρ is 'free charge' that we will associate with NPs.

The nonlinearity of this equation generates great difficulty in solving it for the complex geometry consisting of spherical NPs interacting with a charged interface. Although numerical solutions can be obtained, the possibility of extracting analytical expressions is still preferable because of the intuition one can develop about the dominating effects. One way around the problem of nonlinearity is to use linear approximation on the exponentials in eq. (1) resulting in the linear Poisson-Boltzmann equation.

$$\nabla^2\phi - k^2\phi = -\frac{\rho}{\epsilon_0\epsilon} \tag{2}$$

where k represents the inverse Debye screening length, given by

$$k = \sqrt{\frac{\nu_i z_i^2 e^2}{\epsilon_0\epsilon kT}} \tag{3}$$

The linear response approximation is expected to reproduce well the interaction at large separation between the NPs and between the NPs and the electrode, even though, at short distances, the discrepancy between the approximate and exact solutions can get larger. At very short distances, however, the continuum approximation could break down and nonlocal dielectric screening may start playing a role. The downside – for photonic applications – that in experiments we are usually not able to bring NPs too close to each other [17] becomes good news for the theoretical description!

Even within the linear regime, calculations proved to be very cumbersome, but full derivations are given in the SI.

The difference in electrostatic properties between the two phases results in two mathematical solutions, one on each side of the interface. They have to match the boundary conditions at the interface, the continuity of electric potential and continuity of the normal component of electric displacement. Apart from dielectric properties, another important difference is that the electrolyte phase contains free charge, in this case in the form of ionised ligands on the surface of NPs. If ϵ_1 and ϵ_2 are the dielectric constant of the electrolyte solvent and the high frequency dielectric constant of the electrode, respectively, and k_1^{-1} and k_2^{-1} their respective screening lengths, the potential obeys the following equations:

$$\nabla^2\phi_1 - k_1^2\phi_1 = -\frac{\rho}{\epsilon_0\epsilon_1} \tag{4}$$

$$\nabla^2\phi_2 - k_2^2\phi_2 = 0 \tag{5}$$

Here the two functions, ϕ_1 and ϕ_2 are expressions for the electric potential in electrolyte and solid electrode, respectively. As the solid phase does not contain any external charge, the right hand side of eq.(2) is zero. The situation when the electrode is charged will be treated separately.

Mathematically, the two boundary conditions can be expressed in cylindrical coordinates as:

$$\phi_1\left(\vec{R}, z=0\right) = \phi_2\left(\vec{R}, z=0\right) \tag{6}$$

$$\epsilon_1 \frac{\partial \phi_1}{\partial z} | z=0 = \epsilon_2 \frac{\partial \phi_2}{\partial z} | z=0 \tag{7}$$

The calculations lead to an expression for Fourier transforms of the two potentials in terms of the Fourier transform of the charge density for the used definitions of Fourier transforms see SI. The result is, therefore, general enough to be used for any free charge distribution occurring in the electrolyte.

$$\tilde{\phi}_1(\mathbf{K}, z) = \frac{1}{2\epsilon_0\epsilon_1\sqrt{K^2+k_1^2}}\left(\int_0^\infty e^{-\sqrt{K^2+k_1^2}|z-z_0|}\tilde{\rho}(\mathbf{K}, z_0)dz_0 + \frac{\epsilon_1\sqrt{K^2+k_1^2}-\epsilon_2\sqrt{K^2+k_2^2}}{\epsilon_1\sqrt{K^2+k_1^2}+\epsilon_2\sqrt{K^2+k_2^2}}\int_0^\infty e^{-\sqrt{K^2+k_1^2}(z+z_0)}\tilde{\rho}(\mathbf{K}, z_0)dz_0\right) \tag{8}$$

$$\tilde{\phi}_2(\mathbf{K}, z) = \frac{\int_0^\infty e^{\sqrt{K^2+k_2^2}z-\sqrt{K^2+k_1^2}z_0}\tilde{\rho}(\mathbf{K}, z_0)dz_0}{\epsilon_0\left(\epsilon_1\sqrt{K^2+k_1^2}+\epsilon_2\sqrt{K^2+k_2^2}\right)} \tag{9}$$

From $\tilde{\phi}_1$ and $\tilde{\phi}_2$ the potential energy of a charge distribution in front of an interface can be written as an integral of these functions over the charge distribution.

$$W = 2\pi^2\int_0^\infty dz\int d\mathbf{K}\tilde{\phi}(\mathbf{K}, z)\tilde{\rho}(-\mathbf{K}, z) \tag{10}$$

Apart from the possibility of getting analytical expressions, the linear Poisson-Boltzmann equation also offers a strategical advantage. If the charge distribution is separated into multiple pieces, the charge density generating the electric field will be the sum of the charge densities of the pieces.

$$\rho = \sum_i \rho_i \tag{11}$$

One can see both from the linear Poisson-Boltzmann equation and from solutions (8) and (9) that the potential depends linearly on the charge density. In other words, the total potential can be written as a sum of the potentials that each free charge domain would generate, independently.

$$\phi = \sum_i \phi_i \tag{12}$$

This also allows the electric field and energy of the system to be separated into multiple contributions. Of course, the validity of this superposition principle is totally based on the linearization of the Poisson-Boltzmann equation: in non-linear theory one cannot decouple different Fourier -harmonics.

For a two-dimensional NP array in front of the interface, the total energy can be divided as follows: image potential energy of one particle, energy of one particle interacting with the net charge on the electrode, and pair interaction energy between particles. When it comes to interacting particles, the pair interaction is the key quantity, as interaction with multiple particles can be written as a pairwise summation of interaction energies.

It is also important to note that $\tilde{\phi}_1$, given in eq. (8) contains two terms. The first term represents the potential of the charge distribution in the bulk electrolyte. The energy given by this term is, by definition, the energy required to build the charge distribution given by $\tilde{\rho}$ out of point charges brought from an infinitely large distance. More importantly, the contribution to the energy determined by this first term does not depend on the distance of the charge distribution from the interface. An easy way to visualize it is by mathematically eliminating the interface ($\epsilon_1 = \epsilon_2$ and $k_1 = k_2$). Such operation affects only the second term (eliminating it!), which means it is the second term that is responsible for the effect of the interface on the potential of the charge distribution and, implicitly, on its energy. This term will be labelled $\delta\tilde{\phi}_1$, and the associated image energy, δW.

$$\delta W = 2\pi^2\int_0^\infty dz\int d\mathbf{K}\delta\tilde{\phi}(\mathbf{K}, z)\tilde{\rho}(-\mathbf{K}, z) \tag{13}$$

3.1.1. Interaction of one particle with the interface

The simplest model to mimic the charge distribution of one particle is to consider it homogeneously distributed over an infinitely narrow spherical shell. In reality, the charge discreteness allows the electric field to penetrate inside the shell, but the separation between the ligands is sufficiently small. The ligands are also undulating, smearing the effect of discreteness. Of course, if only a small part of ligands is ionized, this approximation may not be accurate, but this case would not be too interesting, as NPs would be prone to aggregation in the bulk. Still, in the case of acidic ligands, on average, there will be no isolated ionised regions on the particle, as the rate of proton rearrangement across the entire surface is very fast.

To write the charge density mathematically, one needs to look at the geometry of the system first. Let us consider a spherical shell, of radius a, which has its centre located at a distance z_0 from the interface, as shown in Fig. 1. If the total charge is q, then the charge density in cylindrical coordinates is

$$\rho(\mathbf{R}, z) = \frac{q}{4\pi a^2}\delta\left(\sqrt{R^2+(z-z_0)^2}-a\right) \tag{14}$$

with a corresponding Fourier transform

$$\tilde{\rho}(\mathbf{K}, z) = \frac{q}{8\pi^2 a}\mathrm{J}_0\left(K\sqrt{a^2-(z-z_0)^2}\right)\Theta\left(a-|z-z_0|\right) \tag{15}$$

Substituting the charge density into the expressions for image potential $\delta\tilde{\phi}_1$, and then into eq. (13) gives the image potential energy as

$$\frac{\delta W}{kT} = N^2\frac{L_B}{2}\left(\frac{\sinh(k_1 a)}{k_1 a}\right)^2\int_0^\infty \frac{KdK}{\sqrt{K^2+k_1^2}}\frac{\epsilon_1\sqrt{K^2+k_1^2}-\epsilon_2\sqrt{K^2+k_2^2}}{\epsilon_1\sqrt{K^2+k_1^2}+\epsilon_2\sqrt{K^2+k_2^2}}e^{-2\sqrt{K^2+k_1^2}z_0} \tag{16}$$

where N is the number of elementary charges on the particle, L_B is Bjerrum length ($=e^2/4\pi\epsilon_0\epsilon_1 kT$) in the electrolyte, and kT is thermal energy. The structure of this formula coincides with the general expression for image

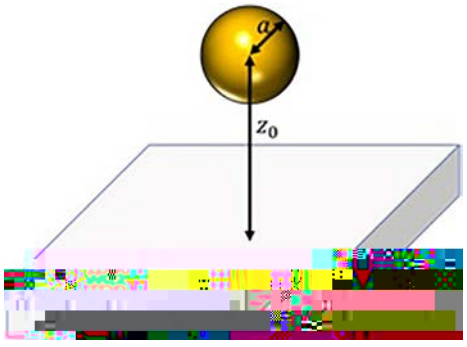

Fig. 1. One NP of radius a, at a distance z_0 from the electrode.

energies at metal-electrolyte interfaces. A very simple limiting case to test this formula is the point charge. Within this limit, the radius of the sphere considered above becomes infinitely small ($a \to 0$), leading to the already known image energy of a point charge near the interface of two plasma-like media [31].

$$\frac{\delta W}{kT} = N^2 \frac{L_B}{2} \int_0^\infty \frac{KdK}{\sqrt{K^2 + k_1^2}} \frac{\epsilon_1 \sqrt{K^2 + k_1^2} - \epsilon_2 \sqrt{K^2 + k_2^2}}{\epsilon_1 \sqrt{K^2 + k_1^2} + \epsilon_2 \sqrt{K^2 + k_2^2}} e^{-2\sqrt{K^2 + k_1^2} z_0} \qquad (17)$$

where β is a constant linked directly to the new screening length, which is yet to be determined.

Even for nonlinear screening, the linearized Poisson-Boltzmann equation will accurately describe the potential and interaction energies in regions where their values are small. The idea behind eq. (25) is to divide the diffuse double layer into a close, fast decaying region (also treated as a linear response decay, but with a much shorter decay length) and a far linear response region with the 'bulk' decay length. Such approach is used to find the renormalized amount of charge that would give the correct far field description.

The nonlinear Poisson-Boltzmann equation was solved, at this stage, numerically using the finite element method in COMSOL Multiphysics. Eq. (25) was fitted with extremely good results to COMSOL simulations. One could calculate, based on acidity constants, pH and ligand sizes, that the total charge on each NP (of the considered 8 nm radius) is about $-870e$. Fig. 3 shows, according to COMSOL, how much of this charge actually contributes to linear screening, concluding that the number is about $-300e$. Therefore, all energies that depend on the total charge are plotted for N_{eff} instead, as it plays the role of a renormalized charge.

In the studied systems we have a high negative charge on the terminal groups of ligands, nonlinearly screened by counterions, leading to a reduced, effective charge (c.f. Debye-Bjerrum approximation). The charge transfer between the electrode and the NPs via the ligands is minor, particularly for positive electrode polarization that attracts NPs to the interface, and for the negatively polarized electrode only via the small portion of ligands adjacent to the electrodes. Thus, this kind of charge transfer could be safely neglected. There may be of course some residual charge on NPs themselves, but it is expected to be minor as compared to the charge of ionized ligands.

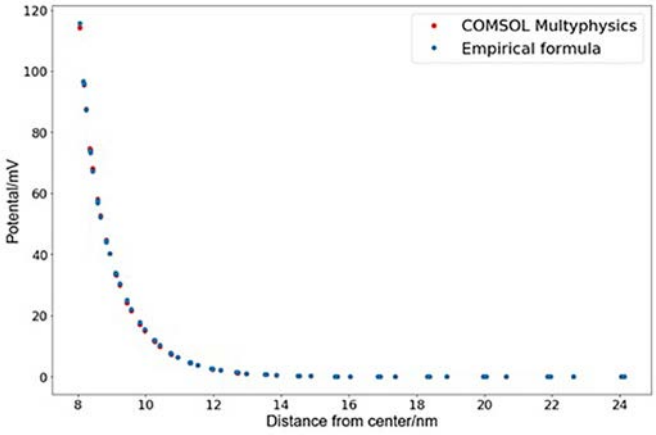

Fig. 3. Electrostatic potential of one NP in the bulk, compared to the empirical formula for potential, with $N_{eff} = 304$, $\beta = 5.767$, $N = 870$, $\epsilon_1 = 79$, a = 8 nm, $k_1 = 0.805\ \mathrm{nm}^{-1}$.

3.1.4. Pair interaction (between two adjacent particles)

The potential of a spherical particle in eq. (8) contains, as mentioned, two terms, only this time both are needed in order to calculate the interaction energy. The first term can be calculated easily in spherical coordinates, leading to

$$\phi_0(r) = \frac{q_1}{4\pi\epsilon_0\epsilon_1}\frac{e^{-k_1 r}}{r}\frac{\sinh(k_1 a)}{k_1 a} \tag{26}$$

where r is the distance from the centre of the particle, $r > a$.

Starting the calculations from the linear version of the Poisson-Boltzmann equation also allows the potential generated by two particles to be written as the sum of individual potentials. Because the model aims at describing a two-dimensional NP array, this interaction will be calculated for two particles located at the same distance from the interface (z_0 surface-to-centre) and separated by a centre-to-centre distance R_0, as in Fig. 4. In this case, the pair interaction energy is given by

$$W = \int d^3\mathbf{r}\phi_0(\mathbf{r})\rho(\mathbf{r}-\mathbf{R_0}) + \int d^3 r\delta\phi(\mathbf{r})\rho(\mathbf{r}-\mathbf{R_0}) \tag{27}$$

Which gives, after a series of manipulations, a closed form expression:

$$\frac{W}{kT} = N^2 L_B\left(\frac{\sinh(k_1 a)}{k_1 a}\right)^2\left(\frac{e^{-k_1 R_0}}{R_0} + \int_0^\infty \frac{KdK}{\sqrt{K^2+k_1^2}}\frac{\epsilon_1\sqrt{K^2+k_1^2}-\epsilon_2\sqrt{K^2+k_2^2}}{\epsilon_1\sqrt{K^2+k_1^2}+\epsilon_2\sqrt{K^2+k_2^2}}e^{-2\sqrt{K^2+k_1^2}z_0}\mathrm{J}_0(KR_0)\right) \tag{28}$$

Its first term represents the interaction energy, within the linear approximation, in the absence of any dielectric interface (or in the bulk, far away from the interface). The second term is a correction caused by the presence of the interface. For an 'ideal' metal (with no static electric field penetration into it), this term is always negative, so inter-particle repulsions are weakened. However, the electrolyte concentration has a much stronger effect on the pair interaction, as one can see in Figs. 5 a) and b).[2]

3.2. Van der Waals interactions

Although tunability is achieved by manipulating electrostatic interactions, van der Waals forces are always present, attracting identical NPs to each other and to the electrode, and electrostatic interactions must be able to compete with them, making the system 'electrovariable'. Strictly speaking, the problem of van der Waals interactions cannot be split into separate contributions (as we did it for the linear PB equation in electrostatics). But a multi-body van der Waals equation would require a very complicated theory [32]. In the linear response approximation, a result for two point like molecules near a metallic surface, which renormalizes the electrostatic Green's function, is known [25]. The result was obtained under the assumption that all characteristic electronic excitations in the substrate metal are much faster than those in the molecules (ideal metal approximation). It shows that the presence of such a substrate diminishes the Heitler-London dispersion forces by a factor of 2/3, if the separation of the molecules from the surface is much smaller than the separation between them. Extension of this result on the case of Van der Waals interaction of NPs and with the account for frequency dependence of the dielectric function of the metal remains to be performed, but a similar kind of reduction is expected to take place there. In this manuscript we deliberately considered the maximal possible effect of Van der Waals interaction, by calculating their van der Waals interactions in the same way as if they were in the

[2] The adsorbed charged species (adatoms or molecules) are known to have Friedel oscillation component in their interaction with each other, mediated by quantum correlations in electron gas of the metal, the effect absent when the metal is treated in classical electrostatics. However, the theoretical investigation of this effect [see the analytical theory in [M.A. Vorotyntsev and A.A. Kornyshev, Electrostatic interaction on a metal insulator interface, Sov.Phys. JETP 51, 509–514 (1980)] has shown that when a point charge is far away (on the atomic scale) compared to the Fermi wave-vector, the effect of Friedel oscillations exponentially decays with the distance from the electrode. Most of the charges on NPs are much farther from the metal surface, so that in our study the effect could be safely neglected.

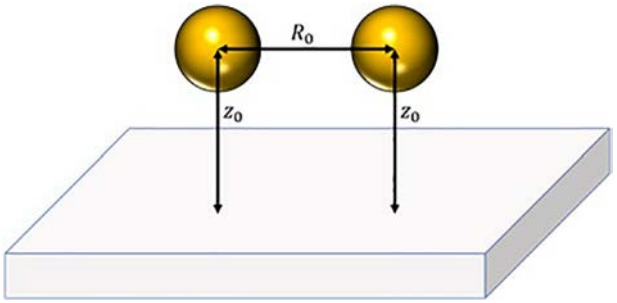

Fig. 4. Pair of NPs separated by a distance R_0, at a distane z_0 from the electrode.

bulk liquid. Mathematically, the chosen approach was the Hamaker-Lifshitz model, which calculates the interaction by summing the interaction energies of induced dipoles. The convenience of this model comes from the fact that van der Waals potential energies are written as a product between an energy constant, calculated from the frequency dependent dielectric response functions, and a geometric factor, which accounts for the shape and separation of the interacting objects [24]. Although formulas are more complicated than those for interactions between atoms, they did not pose any technical problems.

3.2.1. NP-electrode attraction

Geometrically, the configuration of one NP near the electrode is modelled simply as a sphere interacting with a flat surface. The Hamaker constant depends on the dielectric constants of the materials, Au for NPs, and for the electrode the material is usually a metal (Au or Ag) or a semi-metallic material (i.e. TiN or ITO). In this case, the formula for potential energy is [24]:

$$W = -\frac{A_{el.material-gold}}{6}\left(\frac{a}{z_0-a}+\frac{a}{z_0+a}+\ln\frac{z_0-a}{z_0+a}\right) \quad (29)$$

Where $A_{el.\ material/gold}$ is the Hamaker constant for interaction between the electrode material and gold. In order to calculate this constant, it is necessary to represent the frequency dependent dielectric constants accurately. The most convenient way of representing them is through a Drude-Lorentz formula, with two Lorenzians [16].

$$\epsilon(\omega) = \epsilon_\infty - \frac{\omega_p^2}{\omega^2+i\gamma_p\omega} - f_1\frac{\omega_1^2}{\omega^2-\omega_1^2-i\gamma_1\omega} - f_2\frac{\omega_2^2}{\omega^2-\omega_2^2-i\gamma_2\omega} \quad (30)$$

Here ω_p and γ_p are the plasma frequency and plasma damping factor, f_i are oscillator strengths for interband transitions, ω_i are resonance frequencies and γ_i are damping factors for their respective interband transitions.

It is especially important for Au and TiN to reproduce interband transitions accurately, because one of them occurs in the visible range. Although experimental data for the refractive index and extinction coefficient of Au are widely available [33], finding the right Drude-Lorentz fitting parameters for TiN proved to be difficult as its optical properties are highly dependent on the Ti:N ratio [34]. Hence, even a slight difference in the deposition method of the film can lead to different reflectance spectra. The simple solution, in the end, was to find fitting parameters that accurately reproduce the reflectance of the interface in the visible region for the sample used in experiments [17].

Table 1, however, shows Drude-Lorentz parameters for bulk Au and TiN. For gold NPs, it is important to correct the model, to account for their finite size. In this case, a difference in dielectric constant arises from

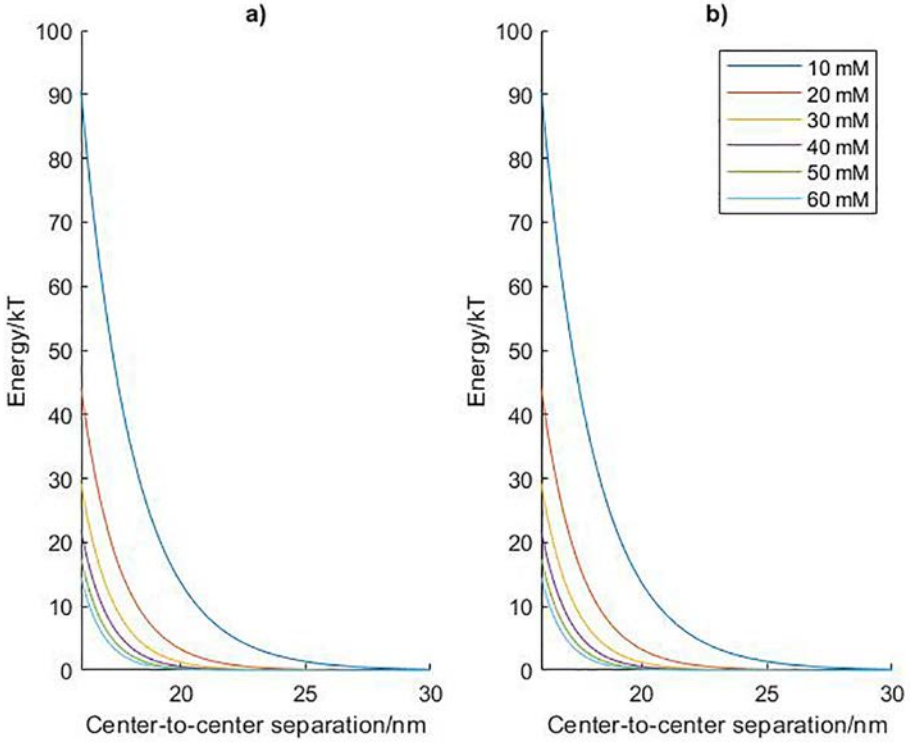

Fig. 5. Pair electrostatic interaction energy of two 8 nm-radius NPs, charged with N = −300 elementary charges, in aqueous electrolyte ($\epsilon_1 = 79$), positioned at a distance of 8.5 nm (center to surface) from a) a gold plate ($\epsilon_2 = 5.92$, $k_2 = 20\ \mathrm{nm}^{-1}$) and b) a TiN plate ($\epsilon_2 = 2.75$, $k_2 = 7.1\ \mathrm{nm}^{-1}$), respectively, as a function of electrolyte concentration. The insets show the colour coding for indicated electrolyte concentrations. Curves are labeled top to bottom. The a) and b) graphs look practically identical due to a very small contribution of image forces at both gold and TiN substrates compared to the head-to-head repulsion; the nature of the metal reveals itself here only in the image forces.

Table 1
Drude-Lorentz fitting parameters for Au and TiN.

	ϵ_∞	ω_p/eV	γ_p/eV	f_1	ω_1/eV	γ_1/eV	f_2	ω_2/eV	γ_2/eV
Au	5.08961	9.0271	0.07595	1.42876	2.95297	0.95409	1.84651	4.06162	1.56389
TiN	1.16671	4.9652	3.05744	2.48806	12.87681	22.40653	4.84377	5.83046	5.2834

the fact that the mean free path of electrons in gold is much larger than the size of a particle. However, this problem can be solved simply by taking the contribution of electron surface scattering [35]. The correction for a spherical particle is then given by:

$$\gamma_p = \gamma_p^{(0)} + \frac{3}{4} A \frac{v_F}{R} \tag{31}$$

where $\gamma_p^{(0)}$ is the plasma damping factor of the bulk material, $A \approx 0.25$ is a constant determined experimentally, v_F is Fermi velocity of electrons in gold, and R is the particle radius.

The purpose behind modelling dielectric constants is to be able to sum over the entire frequency range to calculate the Hamaker constants by summing over the Matsubara frequencies $\omega = 2\pi\,(kT/\hbar)$.

$$A_{el.material-gold} = \frac{3kT}{2} \sum\nolimits'_{n=0,\infty} \left[\frac{\epsilon_{gold}(n) - \epsilon_{water}(n)}{\epsilon_{gold}(n) + \epsilon_{water}(n)}\right] \left[\frac{\epsilon_{el.material}(n) - \epsilon_{water}(n)}{\epsilon_{el.material}(n) + \epsilon_{water}(n)}\right] \tag{32}$$

where the prime indicates that the $n = 0$ term is weighted by 1/2. Results of the Hamaker model are shown for a metal electrode (Au) and for TiN in Figs. 6 a) and b).

3.2.2. Pair interaction

The strategy for calculating attraction between two gold NPs is similar to what was presented in the previous subsection, in the sense that the Hamaker constant is calculated in the same way. The only difference is that both particles are made of gold, so eq. (31) has to be updated to:

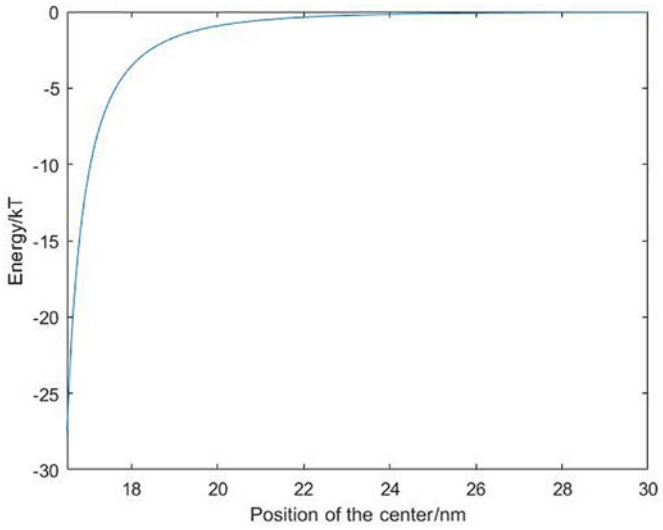

Fig. 7. Van der Waals attraction between two gold NPs, 8 nm in radius, where the gold dielectric constant was calculated with parameters from Table 1.

$$A_{gold-gold} = \frac{3kT}{2} \sum_{n=0}^{\infty}{}' \left(\frac{\epsilon_{gold}(n) - \epsilon_{water}(n)}{\epsilon_{gold}(n) + \epsilon_{water}(n)}\right)^2 \tag{33}$$

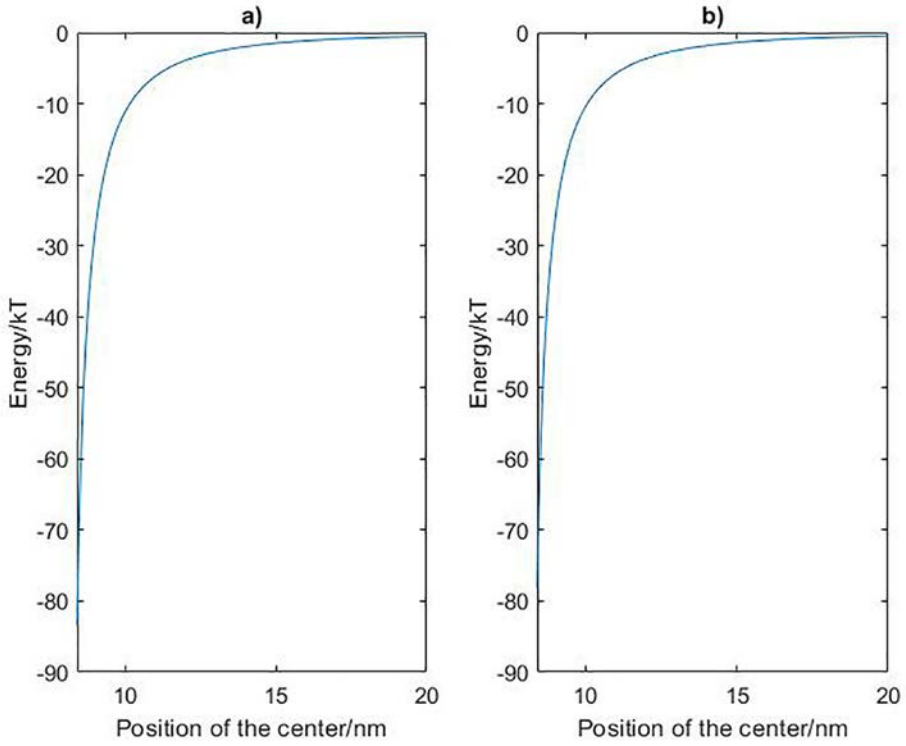

Fig. 6. Van der Waals attraction between one 8 nm-radius particle and a gold (a)/TiN (b) plate, where dielectric constants were evaluated from eq. with Drude-Lorentz parameters from Table 1. The difference between (a) and (b) graphs is tiny due to very close values of Hamaker constants for the two substrates, as calculated via eq. 32 using parameters listed in Table 1: 29.7 kT for Au-Au and 27.8 kT for Au-TiN.

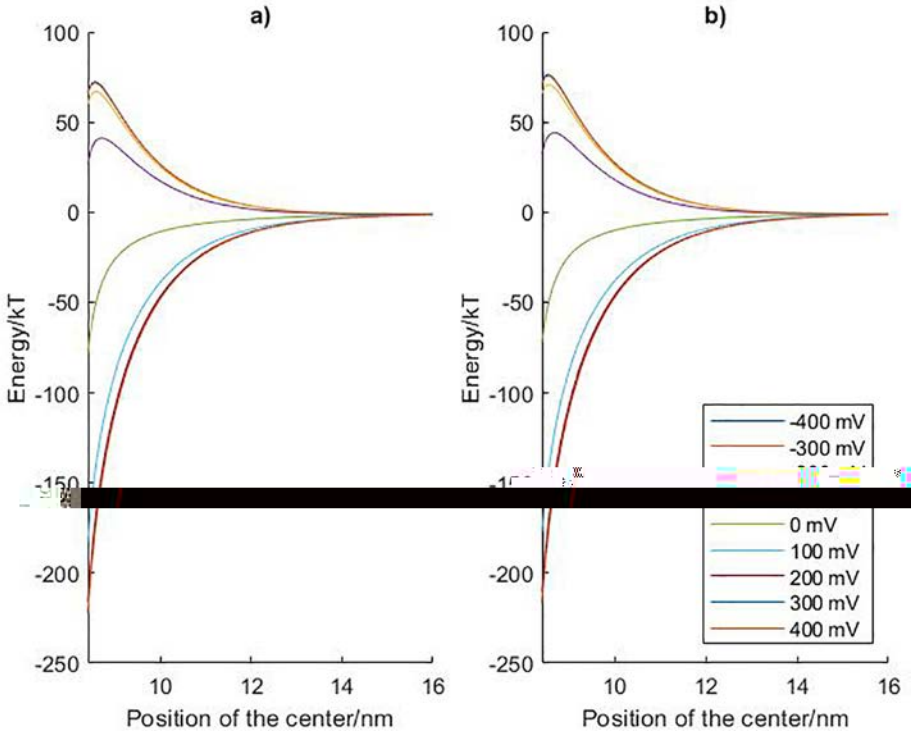

Fig. 8. Total interaction energy between one negatively charged NP and the interface as a function of applied voltage, calculated by adding the van der Waals contribution (as presented in Fig. 6) to the electrostatic contribution, for a gold (a) and TiN (b) substrate. The electrostatic parameters corresponding to the above curves are $\epsilon_2 = 5.92$, $k_2 = 20\ \mathrm{nm}^{-1}$ for gold and $\epsilon_2 = 2.75$, $k_2 = 7.1$ for TiN. The NP, 8 nm in radius, is charged with -300 e, and immersed in a 60 mM electrolyte, with $\epsilon_1 = 79$ and $k_1 = 0.805\ \mathrm{nm}^{-1}$. Curves are labeled top to bottom, with the top 2 and bottom 3 practically overlapping. The tiny difference between graphs a) and b) comes from the proximity of the image and van der Waals forces for the two substrates (see comments in captions to Figs. 5 and 6).

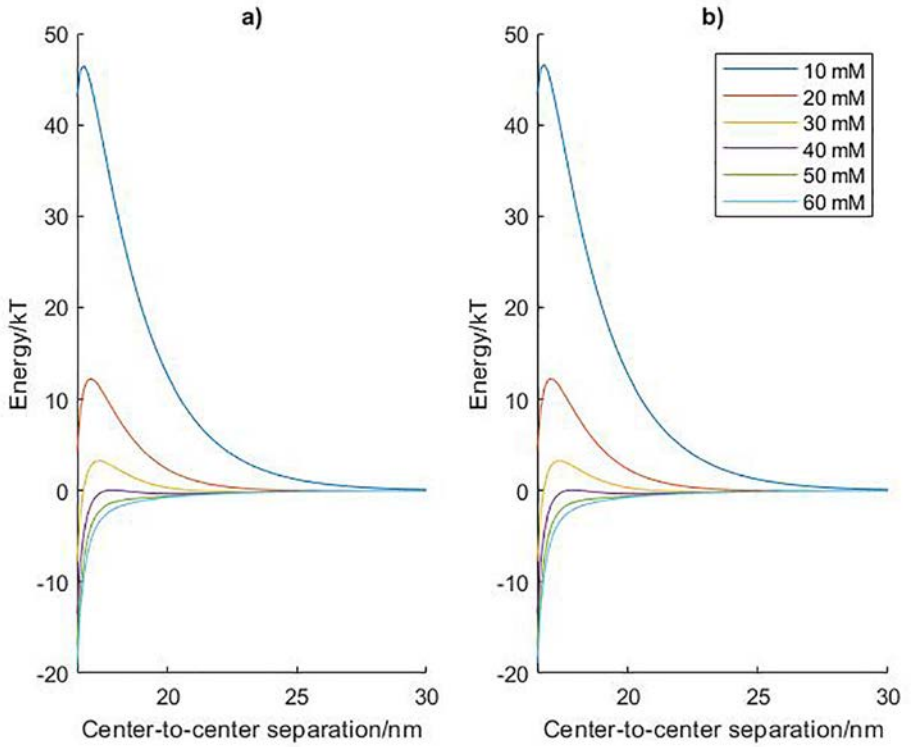

Fig. 9. a) Interaction energy between two NPs as a function of their center-to-center separation, in aqueous solutions at a) gold and b) TiN electrodes, shown for different electrolyte concentrations. All parameters as in Fig. 5. The graphs are calculated by adding the van der Waals contribution (as presented in Fig. 7) to the electrostatic contribution shown in Fig. 5.

where again the $n = 0$ term is weighted by 1/2. Nevertheless, the geometric factor of the interaction has to be changed. Because, this time, the second object is also spherical and is of the same radius, a different version of eq. (32) is required.

$$W = -\frac{A_{gold-gold}}{3}\left[\frac{a^2}{R_0^2-4a^2}+\frac{a^2}{R_0^2}+\frac{1}{2}\ln\left(1-\frac{4a^2}{R_0^2}\right)\right] \tag{34}$$

Applying the formula above gives a van der Waals pair interaction that is, of course, independent of any distance from the interface, according to the aforementioned simplification (in reality, as mentioned, their proximity to the conducting substrate will weaken the Van der Waals interaction).

4. Results and discussion

4.1. Net potential energy profile for NP-electrode interaction

Adding all interactions of one particle with the interface reveals an expected trend concerning electrosorption of a single particle. Even though energy values might not be accurate, Fig. 8 suggests there is enough freedom to vary electrode potentials around the potential of zero charge in order to switch the overall force on each NP from attractive to repulsive.

4.2. Net pair interaction energy

Similarly, all contributions to the pair interaction are also combined. The concentration effect is clear from Fig. 9, the higher the concentration the lower the repulsion. The repulsion is strong enough to win over van der Waals attraction and stop the particles from agglomerating into clusters for electrolyte concentrations of no more than 20 mM. This is actually lower than has been experimentaly observed in ref. 17. The reason is that, as mentioned, the model exaggerated the contribution of van der Waals attraction at electrodes by not taking into account the corresponding contribution of the electrode.

4.3. Mean-field electrosorption isotherm

After developing a consistent model for the key interactions in the system (both van der Waals and electrostatic), one may ask a question, how do these forces affect together the NP assembly at the surface, when it becomes favourable? To answer it, we will analyze the stability of the NP array using the Ising model [22] in the format appropriate for adsorption.

The first assumption that we will make is that NPs, when adsorbed at the interface, arrange themselves into a hexagonal lattice, so all particles will be equally spaced. Next, because electrostatic interactions are exponentially screened, as well as Van der Waals interactions decay no slower than inverse cube of the distance between NPs (which is short range in two dimensions), we can safely take into account only the nearest neighbour interactions. This collapses all pair interaction parameters into one, J, containing both electrostatic and van der Waals contributions at distances between NP corresponding to their dense packing. The fact that practically NPs will settle, if adsorbed, at some distances from each other, will be taken into account through the value of the *coverage*, θ – the probability that a site of that lattice is occupied, $0 < \theta < 1$: the more sparsely the NPs settle at the interface, the lower θ will be. Because the interface interacts in the same way with all particles we can introduce a single parameter, h, which has a meaning of the interaction energy between a NP and the interface; it will contain the contributions from van der Waals attraction, image force, and interaction with the charge on the electrode.

Thus, each site of this isotropic NP lattice (with N being the total number of sites) can be either occupied or unoccupied. As it is done in the 'adsorption version' of the Ising model it is convenient to operate with the 'occupation' variables for each lattice site i. Its values are, in this case, $B_i \in \{0,1\}$. Then the Hamiltonian of the adsorption system reads

$$H = J\sum_{i=1}^{N}\sum_{j\in neighbours(i)} B_iB_j + h\sum_{i=1}^{N} B_i \tag{35}$$

For two adjacent lattice sites, an interaction occurs only if they are both occupied, with $J > 0$ describing the strength of repulsion. Similarly, the interface only interacts with an occupied lattice site.

There is no exact analytical solution for the two-dimensional Ising model in external field (the 'h-term'). For our estimates it would be sufficient, however, to use the simpler, mean-field approximation. In other words, each site is assumed to interact with the average occupancy of the entire lattice, so the Hamiltonian becomes

$$H = (zJ\langle B\rangle + h)\sum_{i=1}^{N} B_i \tag{36}$$

The final step in the Ising model calculation is to find the average value of the occupancy, which represents the coverage of the surface (as a fraction of the number of occupied lattice sites) for a given lattice constant. Considering that occupancies obey the Boltzmann distribution, $\langle B\rangle$ can be written as

$$\langle B\rangle = \frac{e^{-\frac{(zJ\langle B\rangle+h)}{kT}}}{e^{-\frac{(zJ\langle B\rangle+h)}{kT}}+1} \tag{37}$$

This well-known equation does not have an analytical solution for $\langle B\rangle$ as a function of h, but there is one for h as a function of $\langle B\rangle$:

$$\frac{h}{kT} = \ln\frac{1-\langle B\rangle}{\langle B\rangle} - Z\frac{J}{kT}\langle B\rangle \tag{38}$$

For given values of J/kT, plotting h/kT vs $\langle B\rangle$ in the interval between 0 and 1, and rotating the coordinate system by 90 degrees, one obtains a graph of the coverage $\langle B\rangle$ as a function of h. Of course, the value of the lattice constant needs to be set in order to evaluate J. The chosen value corresponds to a relatively dense lattice, where the surface-to-surface separation between NPs is 2 nm. The resulting graphs are shown in Fig. 10 for metallic and semi-metallic electrodes, in which the values of J have been calculated using Eqs. (28) and (34), and h related to voltage subject to Eqs. (17), (22) and (29), each equation representing a separate contribution.

For both types of electrode, theory predicts a very narrow voltage interval (about 30 mV), where the assembly of each lattice changes from unfavourable to favourable. Apart from the conceptual shortcomings of the oversimplified theory presented above, it is also possible that the narrow voltage window for such a transition, which is seen to be significantly larger in experiments [17], may come from different sources – some surface roughness, dispersion in particle sizes, inhomogeneity of lattices-multiple reasons. The neglect of nonlinear effects can generate exaggerated interaction energy values, while in practice, energies could be smaller, entropy widening the voltage interval where assembly takes place. Another point to note, is the difference between the electrosorption isotherms for the two electrodes. As discussed above, the differences in the interaction parameters are small. The difference between the electrosoption curves is not large either - some 10 mV shift, but still noticeable. Both the pair interaction and interaction with the interface have large values relative to thermal energy, and when they are closely balancing each other the tiny differences between the interaction parameters for the two electrodes could give rise to noticeable differences in adsorption isotherms.

Theoretical predictions on the density of NP arrays are given in the form of electrosorption isotherms. Changing the potential drop across the interface can easily shift the balance between pair interaction and NP-electrode interaction, allowing particles to assemble or disassemble. However, the simplicity of the theoretical framework is likely to give inaccurate numerical results, while giving a good qualitative picture. In order to solve this problem or, at least, improve the estimates, one has to return to the

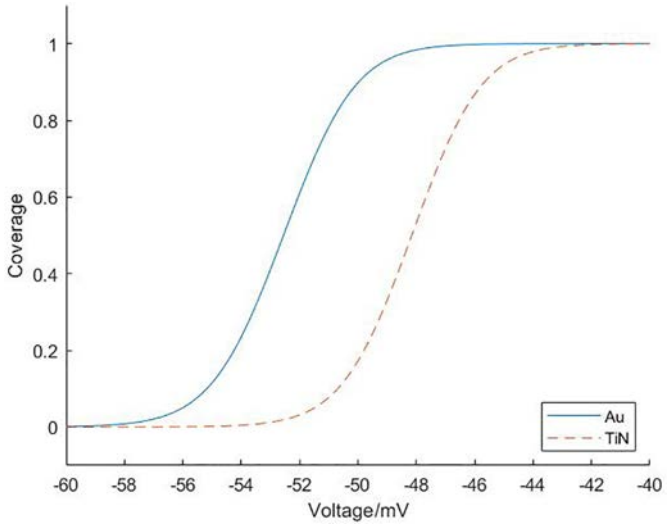

Fig. 10. Electrosorption isotherm: lattice coverage as a function of applied potential, calculated vs potential of zero charge, for Au and TiN substrates, based on the interaction energies shown in Figs. 8 and 9, evaluated for a lattice constant of 19 nm and particle centers at 8.5 nm from the interface. Note that each of the electrodes has its own pzc, and they are different. So voltage here means the deviation from each pzc. The experiments of Ref.17 reveal the qualitatively similar curve for TiN-film-covered Ag electrode but the transition from full to zero coverage is much less steep for the reasons discussed in the text.

assumptions behind electrostatic forces. Regarded as an important correction would be the fact that NPs are polarisable. So, the pair interaction, for example, has to take into account that each charged particle polarises the other particles around it. This problem was solved to some degree [36], (within linear Poisson-Boltzmann regime) but the problem of nonlinear effects still remains. Equally on the Van der Waals front, it would be better to take into account the effect of the substrate on pair interactions. But this may be of lower importance, because, as we see, the Van der Waals interactions are generally substantially smaller than the electrostatic ones, unless we screen the latter stronger, by electrolyte concentrations higher than those considered in this study.

5. Conclusion

The analysis presented in this study highlights the following effects influencing assembly or disassembly of NP arrays at electrochemical solid-liquid interfaces:

1. Interaction energies of NPs with the interface are highly dependent on applied voltage
2. Van der Waals and image forces tend to combine into a force attracting each NP to the interface
3. The pair electrostatic interaction energy does not depend on the applied voltage,but is largely influenced by electrolyte concentration through screening. This is true, of course, only within the considered approximations - in reality the compression of the double layer with larger charges of the electrode can alter the effective screening of the pair interaction between NPs. Had we taken into e.g., account the increase of concentration of counterions of the same sign as of NPs (considered to be negative in this work), we would have stronger repulsion between them for positive electrode polarisations and a weaker repulsion for negative ones, which would have smoothened the coverage dependence on electrode potential, increasing the voltage range where the crossover between assembly and disassembly would take place.

But all in all, we have shown that the reversible assembly at the solid-liquid interface is made possible simply by changing the voltage applied across the interface, as we have seen in optical experiments [17].

Declaration of Competing Interest

None.

Appendix A. Supplementary information

on line: https://doi.org/10.1016/j.jelechem.2020.114275. It contains the details of derivation of the electrostatics formulae and the dielectric functions of the materials involved. Supplementary data to this article can be found online at https://doi.org/10.1016/j.jelechem.2020.114275.

Acknowledgements

AAK acknowledges the EPSRC grant EP/L02098X/1 and CZ the stipend from the EPSRC grant EP/L015579/1.

References

[1] B. Luk'yanchuk, N.I. Zheludev, S.A. Maier, N.J. Halas, P. Nordlander, H. Giessen, C.T. Chong, Nat. Mater. 9 (2010) 707–715.
[2] N.I. Zheludev, Y.S. Kivshar, Nat. Mater. 11 (2012) 917–924.
[3] J.Y. Ou, E. Plum, L. Jiang, N.I. Zheludev, Nano Lett. 11 (2011) 2142–2144.
[4] Z. Fei, A.S. Rodin, G.O. Andreev, W. Bao, A.S. McLeod, M. Wagner, L.M. Zhang, Z. Zhao, M. Thiemens, G. Dominguez, M.M. Fogler, A.H.C. Neto, C.N. Lau, F. Keilmann, D.N. Basov, Nature 487 (2012) 82–85.
[5] J. Gu, R. Singh, X. Liu, X. Zhang, Y. Ma, S. Zhang, S.A. Maier, Z. Tian, A.K. Azad, H.-T. Chen, A.J. Taylor, J. Han, W. Zhang, Nat. Commun. 3 (2012) 1151.
[6] I.V. Shadrivov, S.K. Morrison, Y.S. Kivshar, Opt. Express 14 (2006) 9344.
[7] Q. Zhao, L. Kang, B. Du, B. Li, J. Zhou, H. Tang, X. Liang, B. Zhang, Appl. Phys. Lett. 90 (2007), 011112. .
[8] R. Singh, E. Plum, W. Zhang, N.I. Zheludev, Opt. Express 18 (2010) 13425.
[9] Y. Yao, R. Shankar, M.A. Kats, Y. Song, J. Kong, M. Loncar, F. Capasso, Nano Lett. 14 (2014) 6526–6532.
[10] D. Shrekenhamer, W.-C. Chen, W.J. Padilla, Phys. Rev. Lett. 110 (2013) 177403.
[11] S. Srivastava, N.A. Kotov, Soft Matter 5 (2009) 1146.
[12] M.E. Flatté, A.A. Kornyshev, M. Urbakh, J. Phys, Chem. C 114 (2010) 1735–1747.
[13] J.B. Edel, A.A. Kornyshev, A.R. Kucernak, M. Urbakh, Chem. Soc. Rev. 45 (2016) 1581–1596.
[14] Y. Montelongo, D. Sikdar, Y. Ma, A.J.S. McIntosh, L. Velleman, A.R. Kucernak, J.B. Edel, A.A. Kornyshev, Nat. Mater. 16 (2017) 1127–1135.
[15] D. Sikdar, A.A. Kornyshev, Sci. Rep. 6 (2016) 33712.
[16] D. Sikdar, S.B. Hasan, M. Urbakh, J.B. Edel, A.A. Kornyshev, Phys. Chem. Chem. Phys. 18 (2016) 20486–20498.
[17] Y. Ma, C. Zagar, D.J. Klemme, D. Sikdar, L. Velleman, Y Montelongo, S.H. Oh, A.R. Kucernak, J.B. Edel, A.A. Kornyshev, ACS Photonics. 5 (2018) 4604–4616.
[18] A.N.J. Rodgers, S.G. Booth, R.A.W. Dryfe, Electrochem. Commun. 47 (2014) 17–20.
[19] M.E. Flatté, A.A. Kornyshev, M. Urbakh, J. Phys. Condens. Matter 20 (2008), 073102.
[20] L. Velleman, D. Sikdar, V.A. Turek, A.R. Kucernak, S.J. Roser, A.A. Kornyshev, J.B. Edel, Nanoscale 8 (2016) 19229–19241.
[21] H. Weir, J.B. Edel, A.A. Kornyshev, D. Sikdar, Sci. Rep. 8 (2018) 565.
[22] K. Huang, Statistical Mechanics, Wiley, 2008.
[23] T. Miura, K. Seki, J. Phys, Chem. B 119 (2015) 10954–10961.
[24] V.A. Parsegian, Cambridge University Press, Van der Waals Forces : a Handbook for Biologists, Chemists, Engineers, and Physicists, Cambridge University Press, 2005.
[25] J. Mahanty, B.W. Ninham, Dispersion Forces, Academic Press, 1976.
[26] M. Marcovitch, H. Diamant, Phys. Rev. Lett. 95 (2005) 223203.
[27] M. Cho, R.J. Silbey, J. Chem. Phys. 104 (1998) 8730.
[28] K. Mathwig, T.J. Aartsma, G.W. Canters, S.G. Lemay, Annu. Rev. Anal. Chem. 7 (2014) 383–404.
[29] A.S. Poulos, D. Constantin, P. Davidson, M. Impéror-Clerc, B. Pansu, S. Rouzière, EPL (Europhysics Lett.) 100 (2012) 18002.
[30] J.N. Israelachvili, Intermolecular and surface forces, Academic Press, 2011.
[31] A.A. Kornyshev, A.I. Rubinshtein, M.A. Vorotyntsev, Phys. Status Solidi 84 (1977) 125–132.
[32] R.A. DiStasio, O.A. von Lilienfeld, A. Tkatchenko, Proc. Natl. Acad. Sci. U. S. A. 109 (2012) 14791–14795.
[33] P.B. Johnson, R.W. Christy, Phys. Rev. B 6 (1972) 4370–4379.
[34] P. Patsalas, N. Kalfagiannis, S. Kassavetis, Materials (Basel). 8 (2015) 3128–3154.
[35] A. Alabastri, S. Tuccio, A. Giugni, A. Toma, C. Liberale, G. Das, F. De Angelis, E. Di Fabrizio, R.P. Zaccaria, Mater. (Basel, Switzerland) **6** (2013) 4879–4910.
[36] H. Ohshima, E. Mishonova, E. Alexov, Biophys. Chem. 57 (1996) 189–203.